International Journal of Scientific Research in Mathematical and Statistical Sciences **Research Paper**
Vol.4, Issue.2, pp.1-13, April (2017) **E-ISSN:** 2348-4519

Stochastic Reynolds Equation for Diverse Shaped Slider Bearing when Lubricated with Couplestress Fluid and by Applying MHD

S. T. Fathima[1] , C.K. Sreekala[2*], B.N. Hanumagouda[3]

[1]West Monroe, Luisiana, USA
[2*]Department of Mathematic, Nitte Meenakshi Institute of Technology, Bangalore, India
[3]Department of Mathematic, Reva University, Bangalore, India

Corresponding Author: tasneemhashmi@gmail.com

Available online at: www.isroset.org

Received 22nd Feb 2017, Revised 04th Mar 2017, Accepted 5th Apr, Online 30th Apr 2017

Abstract- Purpose- The objective of this paper is to conduct a theoretical analysis of wide composite slider bearings of diverse film shapes like parabolic, plane, exponential, and secant for the case of couplestress fluid in the existence of magnetic field applied normal to bearing surface and on the basis of roughness of the surface.
Design/Methodology – The generalised stochastic Reynolds equation is derived based on Stokes model and Christensen stochastic model. The expressions for the characteristics of bearing are obtained for general lubricant film shape in integral form and are numerically computed for the shapes under consideration.
Findings- It is fascinating to note that the impact of magnetic field, couplestress and roughness of surface significantly affect the bearing characteristics. It is concluded from comparison that load supporting capability of parabolic slider is more significant.
Originality/value – It is expected that these analyses will help design engineers to choose proper shaped slider bearings with appropriate couplestress, roughness parameters in the occurrence of applied magnetic field, which improves the normal functioning of the bearings.

Keywords: Composite slider, Couple-stress fluid, Surface roughness, Magnetic field

I. INTRODUCTION

In this paper, the expression for Stochastic Reynolds equation is derived and a comparative study is made to analyse the combined impact of MHD, couplestress and surface roughness on different shapes of film (viz., parabolic, plane, exponential, and secant).
In this article section-I contains introduction, section-II contains related work, section-III contains mathematical formulation and methodology, section-IV contains results and discussion and section-V contains conclusion.

II. RELATED WORKS

Slider bearings are frequently designed to support the axial-component thrust in a rotating shaft. The knowledge about the characteristics of bearing making into note of various operating circumstances is critical. Over recent years numerous established analysis has been finalized on lubrication performance of slider bearings. Later to upgrade the lubricating performance the increased utilization of Newtonian lubricant which has been blended with long chain polymers has been observed. It imparts most necessary properties of the fluid. The usage of additives steadies the flow properties and minimises the sensitivity of lubricant to change in shear rate. A variety of microcontinuum theories have been suggested by Ariman et.al [1-2] and applied in lubrication problems such as continuum model of micro polar fluids [3]. Stokes [4] suggested the simplest micro-continuum theory which permits the occurrence of Couple stresses and body couples. The load supporting capability, force of friction increases and frictional coefficient decreases for a slider bearing greased with couplestress fluid was concluded by Ramanaiah and Sarkar [5]. A comparative study is made between parabolic and inclined slider lubricated with couplestress fluid by Moobalaji and John [7] and found that parabolic slider has more superior load supporting capability than inclined slider. The consequence of MHD has been considered for different film shapes by Lin et.al [8-12] and found development in bearing characteristics with increase of magnetic field.

The combined effect of MHD and Couplestress has been studied for different bearings by Naduvinamani et.al [13], Biradar and Hanumagowda [14] and on different types of plates by Fathima et.al [15-16] and they found that these effects are more significant in the load supporting capability.

A small variation in height distribution, width and curvature of asperity peaks can have a significant impact on bearing performance. In recent years, a considerable work is being devoted to analyse the importance of roughness of surface on the mean pressure and mean load supporting capacity of bearing in fluid dynamic lubrication. Christensen [17] developed stochastic models for hydrodynamic lubrication of rough surfaces. By using this model, Naduvinamani and co-workers [18-23] have extensively studied the impact of roughness on the surface of distinctive bearing system lubricated with non-Newtonian fluids.

III. Mathematical formulation

Figure (1-3) shows the diagram of the designs under study. The bearing is of length L. It comprises of two surfaces. The lower surface of the bearing taken along x-axis is running with a constant velocity U in its own plane while the upper surface is at rest and is taken along z-axis. The surface of the bearing is assumed as rough. The magnetic field is applied perpendicular to the surface. Film thickness equations of the bearings under consideration are

For parabolic slider $h(x) = h_0 + d(1 - 2\frac{x}{L} + \frac{x^2}{L^2})$ (1)

For plane slider $h(x) = h_0 + d(1 - \frac{x}{L})$

For secant slider $h(x) = h_0 Sec\left\{d\left(1 - x/L\right)\right\}$ (3)

Where $d = Sec^{-1}\left(\delta + 1\right)$

For exponential slider $h(x) = h_0 \exp\left\{-(x/L)\ln\frac{h_1}{h_0}\right\}$ (4)

The equations governing the flow are

$$\frac{\partial u}{\partial x} + \frac{\partial w}{\partial z} = 0 \quad (5)$$

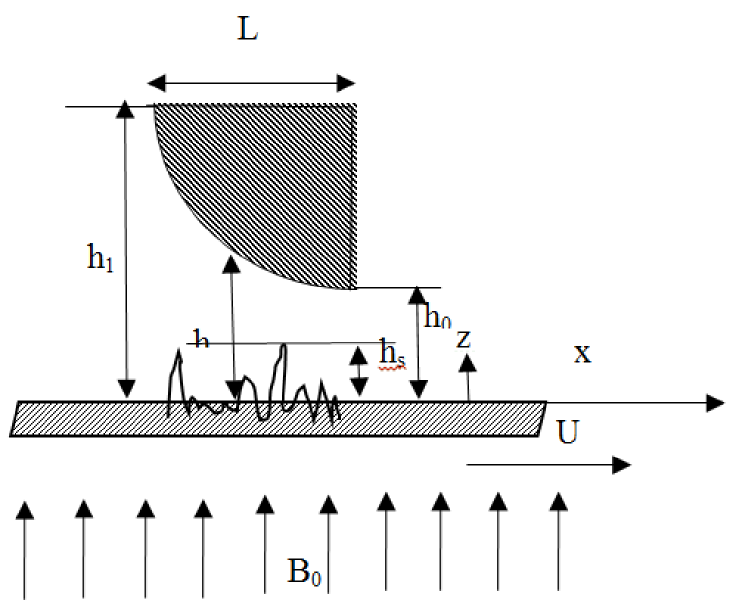

Fig.1 Geometry of rough exponential and secant slider bearing

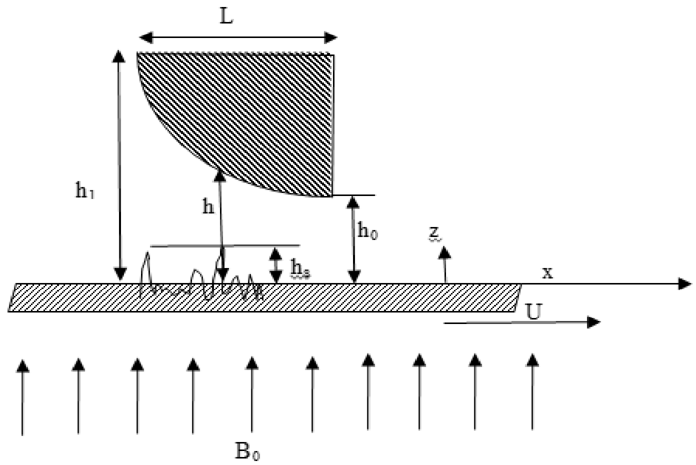

Fig. 2 Geometry of rough parabolic slider bearing

$$\mu\frac{\partial^2 u}{\partial z^2}-\eta\frac{\partial^4 u}{\partial z^4}-\sigma B_0^2 u=\frac{\partial p}{\partial x}+\sigma E_y B_0 \tag{6}$$

$$\frac{\partial p}{\partial z}=0 \tag{7}$$

The no-slip boundary conditions are; At the upper surface $z=H$

$$u=0 \qquad \frac{\partial^2 u}{\partial z^2}=0 \qquad w=0 \tag{8}$$

At the lower surface $z=0$

$$u=U \qquad \frac{\partial^2 u}{\partial z^2}=0 \qquad w=0 \tag{9}$$

Where u, v, w are component of velocity in x, y, z directions respectively.
Solving equation (6) together with boundary conditions (8) and (9) gives the component of velocity as

$$\begin{aligned}\therefore u=&-\frac{B^2}{(A^2-B^2)}\frac{h_0^2}{\mu M_0^2}\left(\frac{\partial p}{\partial x}+\sigma E_y B_0\right)\left(Cosh\frac{Az}{l}-\tanh\frac{AH}{2l}Sinh\frac{Az}{l}-1\right)\\&-\frac{B^2U}{(A^2-B^2)}\left(Cosh\frac{Az}{l}-\coth\frac{AH}{l}Sinh\frac{Az}{l}\right)\\&+\frac{A^2}{(A^2-B^2)}\frac{h_0^2}{\mu M_0^2}\left(\frac{\partial p}{\partial x}+\sigma E_y B_0\right)\left(Cosh\frac{Bz}{l}-\tanh\frac{BH}{2l}Sinh\frac{Bz}{l}-1\right)\\&+\frac{A^2U}{(A^2-B^2)}\left(Cosh\frac{Bz}{l}-\coth\frac{BH}{l}Sinh\frac{Bz}{l}\right)\end{aligned} \tag{10}$$

Where $A=\sqrt{\left(\frac{1+\sqrt{1-4l^2M_0^2/h_0^2}}{2}\right)}$ and $B=\sqrt{\left(\frac{1-\sqrt{1-4l^2M_0^2/h_0^2}}{2}\right)}$

If the surfaces of the bearing are flawless protectors and there is circuit exterior to the fluid film, then the electric field may be approximated by requiring the net current stream to be zero.

$$\int_{y=0}^{h}\left(E_y+B_0u\right)dz=0 \tag{11}$$

Solving equations (10) and (11) we get

$$u=-\frac{h_0^2}{\mu M_0^2}\frac{\partial p}{\partial x}\frac{H}{2l}\left[\frac{A^2\left\{\dfrac{Sinh\frac{BH}{l}-Sinh\frac{Bz}{l}-Sinh\frac{B(H-z)}{l}}{\left(Sinh\frac{BH}{l}\right)}\right\}-B^2\left\{\dfrac{Sinh\frac{AH}{l}-Sinh\frac{Az}{l}-Sinh\frac{A(H-z)}{l}}{\left(Sinh\frac{AH}{l}\right)}\right\}}{\frac{A^2}{B}\tanh\frac{BH}{2l}-\frac{B^2}{A}\tanh\frac{AH}{2l}}\right] \qquad (12)$$

$$+\frac{U}{2(A^2-B^2)}\left\{-B^2\left(\frac{Sinh\frac{AH}{l}-Sinh\frac{Az}{l}+Sinh\frac{A(H-z)}{l}}{Sinh\frac{AH}{l}}\right)+A^2\left(\frac{Sinh\frac{BH}{l}-Sinh\frac{Bz}{l}+Sinh\frac{B(H-z)}{l}}{Sinh\frac{BH}{l}}\right)\right\}$$

Subject to the conditions (8) and (9), and making use of equation (12) in (5) and integrating we get one dimensional modified Reynolds equation in the form

$$\frac{\partial}{\partial x}\left[f(H,l,M_0)\frac{1}{\mu}\frac{\partial p}{\partial x}\right]=6U\frac{dH}{dx} \qquad (13)$$

Where $f(H,l,M_0)=\dfrac{6H^2h_0^2}{lM_0^2}\left\{\dfrac{\left(A^2-B^2\right)}{\frac{A^2}{B}\tanh\frac{BH}{2l}-\frac{B^2}{A}\tanh\frac{AH}{2l}}-\dfrac{2l}{H}\right\}$ (14)

The thickness of film is comprised of two parts

$$H=h(x)+h_s(x,\xi) \qquad (15)$$

In common two types of roughness structures are of importance. But our investigation is limited to only one- dimensional longitudinal roughness, because, the longitudinal roughness and the transverse roughness can be made same, by just a rotation of co-ordinate axes.

Taking expectation on both sides of equation (13) and by applying Christensen stochastic approach for rough surfaces, Stochastic Reynolds equation for longitudinal roughness takes the form.

$$\frac{\partial}{\partial x}\left[\frac{\partial E(p)}{\partial x}\frac{1}{\mu}E\left\{f(H,l,M_0)\right\}\right]=6U\frac{dE\left(H\right)}{dx}$$

(16) $E(*)$ is defined by

$E(*)=\int_{-\infty}^{\infty}(*)\,f(h_s)dh_s$ Where $f(h_s)$ is the p.d.f of the random variable h_s. The rough surfaces in engineering application are of Gaussian type and hence, the below cited polynomial function is chosen to approximate the Gaussian distribution;

By Christensen (1969-1970) theory we assume that

$$f(h_s)=\begin{cases}\dfrac{35}{32c^7}(c^2-h_s^2)^3. & -c<h_s<c\\ 0 & elsewhere\end{cases}$$

Therefore $E(f(H,l,M_0))=\dfrac{35}{32c^7}\displaystyle\int_{-c}^{c}f(H,l,M_0)(c^2-h_s^2)^3\,dh_s$

$$E\left(\frac{1}{f(H,l,M_0)}\right)=\frac{35}{32c^7}\int_{-c}^{c}\frac{(c^2-h_s^2)^3}{f(H,l,M_0)}dh_s$$

$$E\left(H\right)=h$$

Introducing non-dimensional quantities to (16)

$$x^* = \frac{x}{L},\ P = \frac{E(p)h_0^2}{\mu UL},\ l^* = \frac{2l}{h_0},\ H^* = \frac{H}{h_0}, h^* = \frac{h}{h_0}, M_0 = B_0 h_0 \left(\frac{\sigma}{\mu}\right)^{1/2}, C = \frac{c}{h_0}$$

$$\frac{\partial}{\partial x^*}\left[\frac{\partial P}{\partial x^*} G^*(H^*, l^*, M_0, C)\right] = 6\frac{dh^*}{dx^*} \tag{17}$$

Where $$G^*(H^*, l^*, M_0, C) = \begin{cases} E(F(H^*, l^*, M_0)) & \text{For longitudinal roughness} \\ \{E(1/(F(H^*, l^*, M_0)))\}^{-1} & \text{For traseverse roughness} \end{cases} \tag{18}$$

And $$F(H^*, l^*, M_0) = \frac{12H^{*2}}{l^* M_0^2}\left\{\frac{(A^{*2} - B^{*2})}{\frac{A^{*2}}{B^*}\tanh\frac{B^* H^*}{l^*} - \frac{B^{*2}}{A^*}\tanh\frac{A^* H^*}{l^*}} - \frac{l^*}{H^*}\right\}$$

Integrating twice with respect to x^*

$$\frac{\partial P}{\partial x^*} G^*(H^*, l^*, M_0, C) = 6h^* + C_1$$

$$\frac{\partial P}{\partial x^*} = \frac{6h^* + C_1}{G^*(H^*, l^*, M_0, C)} \tag{19}$$

$$P = 6\int_{x^*=0}^{x^*} \frac{h^*}{G^*(H^*, l^*, M_0, C)} dx^* + C_1 \int_{x^*=0}^{x^*} \frac{1}{G^*(H^*, l^*, M_0, C)} dx^* + C_2 \tag{20}$$

The boundary conditions are $P = 0$ at $x^* = 0, \alpha$

Where ; $\alpha = \{1,$ For parabolic, plane and secant, hyperbolic slider

And $\alpha = \{-1,$ For exponential slider

Applying the boundary conditions and solving Equation (20) we have

$$P = \int_{x^*=0}^{x^*} \frac{6(h^* - \psi)}{G^*(H^*, l^*, M_0, C)} dx^* \tag{21}$$

Where $$\psi = \frac{\int_{x^*=0}^{\alpha} \frac{h^*}{G^*(H^*, l^*, M_0, C)} dx}{\int_{x^*=0}^{\alpha} \frac{1}{G^*(H^*, l^*, M_0, C)} dx^*}$$

The dimensionless load supporting capability is

$$W^* = \frac{E(w)h_0^2}{\mu UL^2} = \alpha \int_0^{\alpha} \int_{x^*=0}^{x^*} \frac{6(h^* - \psi)}{G^*(H^*, l^*, M_0, C)} dx^* dx^* \tag{22}$$

The non- dimensional frictional force is $$F^* = \alpha \left\{ \begin{array}{l} \int_0^{\alpha} E(G^*(H^*, l^*, M_0)) dx^* + 3\int_0^{\alpha} E\left\{\frac{H^*}{\xi(H^*, l^*, M_0)}\right\} dx^* \\ -3E\left\{\frac{\int_{x^*=0}^{\alpha} \frac{H^*}{F^*(H^*, l^*, M_0)} dx^*}{\int_{x^*=0}^{\alpha} \frac{1}{F^*(H^*, l^*, M_0)} dx^*}\right\} \int_0^{\alpha} E\left(\frac{1}{\xi(H^*, l^*, M_0)}\right) dx^* \end{array} \right\}$$

(23)

Where $\xi(H^*,l^*,M_0)=\frac{12H^*}{l^*M_0^2}\left\{\frac{\left(A^{*2}-B^{*2}\right)}{\frac{A^{*2}}{B^*}\tanh\frac{B^*H^*}{l^*}-\frac{B^{*2}}{A^*}\tanh\frac{A^*H^*}{l^*}}-\frac{l^*}{H^*}\right\}$

And $G(H^*,l^*,M_0)=\frac{l^*M_0^2}{4(A^{*2}-B^{*2})}\left(\frac{A^{*2}}{B^*}\coth\frac{B^*H^*}{l^*}-\frac{B^{*2}}{A^*}\coth\frac{A^*H^*}{l^*}\right)$

The coefficient of friction $\chi=\frac{F^*}{W^*}$ (24)

IV. METHODOLOGY

The expression for load supporting capability, force of friction and frictional coefficient is evaluated using mathematic software and the integrals are evaluated numerically using Simpsons one-third rule.

V. RESULT AND DISCUSSION

The study about the collective impact of magnetic field, on rough slider bearing of diverse film shapes greased with couplestress fluid is presented in this paper. The characteristics of the bearing are attained as functions of roughness parameter C, couple stress parameter l^*, Hartmann number M_0. The table represent performance characteristics of slider bearing having film profiles viz., parabolic, plane, exponential, and secant.

Figures 4 and 5 represent the changes in normalised load supporting capability due to longitudinal and transverse roughness striations of various sliders against the shoulder parameter. It is fascinating to note that in the presence of applied magnetic field, rough parabolic slider is having superior load supporting capability in comparison with other sliders.

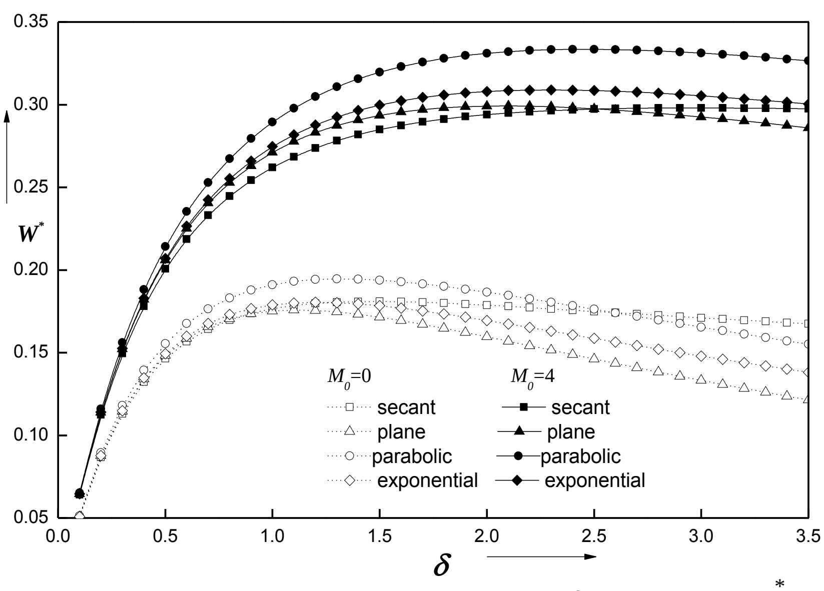

Fig. 4 Graph depicting longitudnal load carrying capacity of distinct sliders when l^*,C=0.3

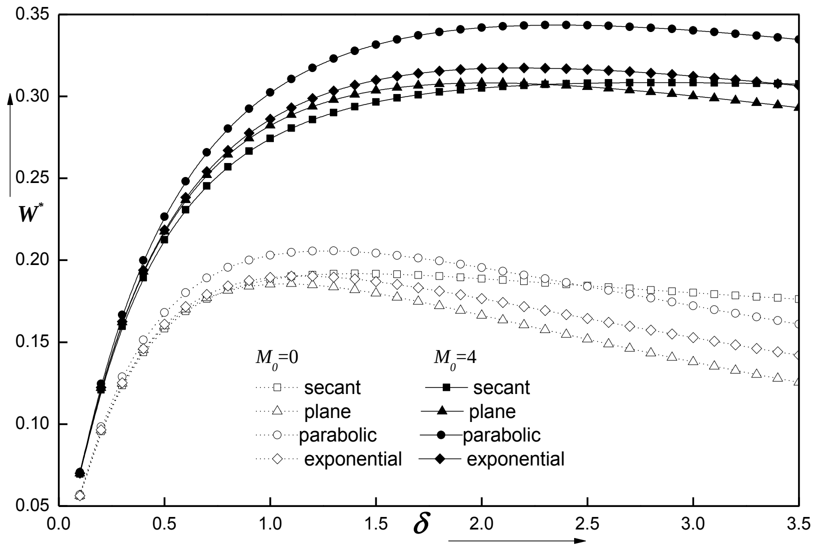

Fig. 5 Graph depicting transverse load carrying capacity of distinct sliders whenl^*,C=0.3

Figures 6 and 7 shows the changes in non-dimensional frictional force for longitudinal and transverse roughness striations for various film shapes greased with couplestress fluid in the occurrence of applied magnetic field.

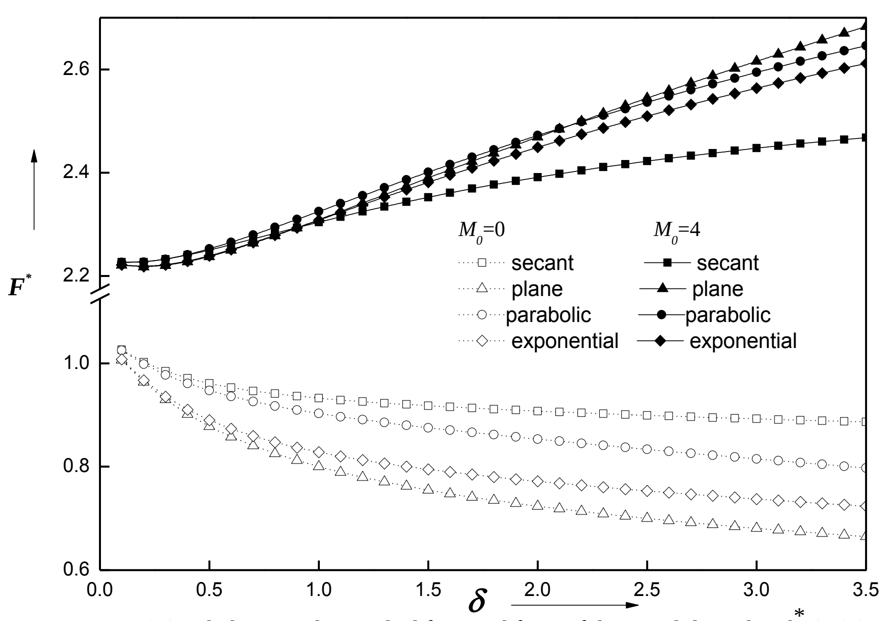

Fig. 6 Graph depicting longitudnal frictional force of distinct sliders when l^*,C=0.3

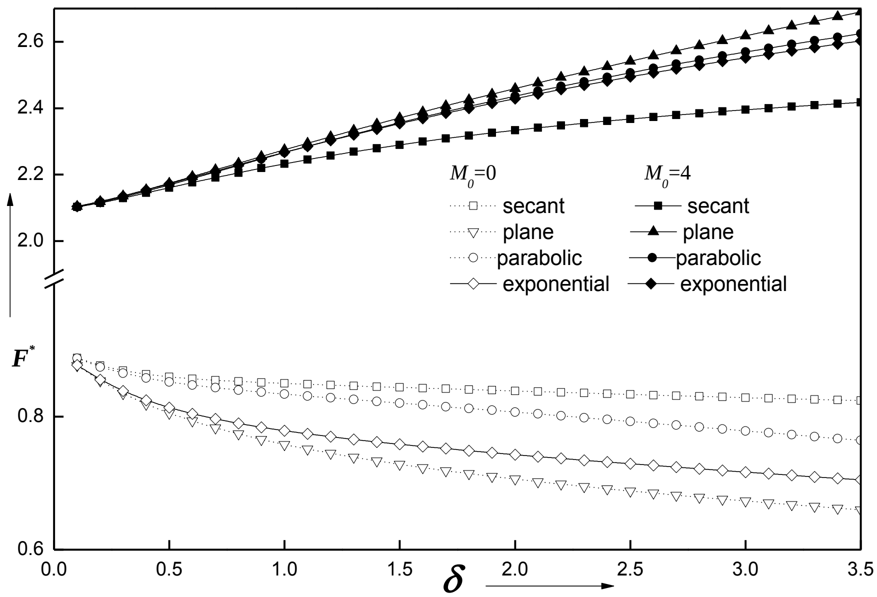

Fig. 7 Graph depicting transverse frictional force of distinct sliders when l^*,C=0.3

Figures 8 and 9 corresponds to graph plotted for frictional coefficient. It is clearly visible that in the occurrence of magnetic field applied perpendicularly, parabolic slider bearing is having lower frictional coefficient than other sliders.

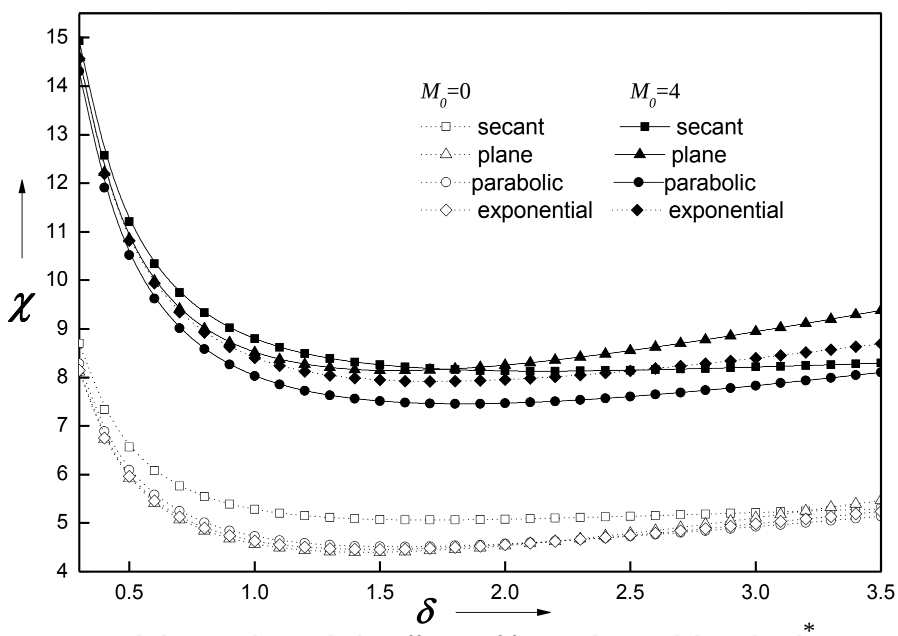

Fig. 8 Graph depicting longitudnal coefficient of friction distinct sliders when l^*,C=0.3

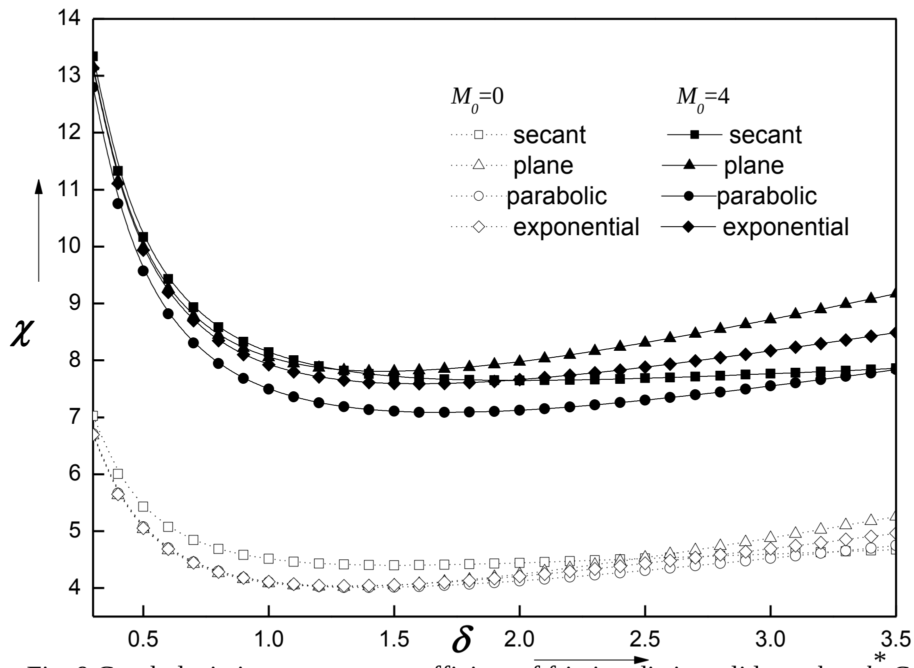

Fig. 9 Graph depicting transverse coefficient of friction distinct sliders when l^*,C=0.3

Table I: represent the changes of normalised load supporting capability of the five sliders when the couple stress parameter is $l^* = 0.3$. It is examined that in smooth case when $C = 0$ both horizontal roughness and vertical roughness coincide. The capacity to support load for vertical roughness is higher than that of smooth case while the longitudinal roughness has reverse trend. From the table, it is trivial that the parabolic slider has significant load supporting capability when compared with other sliders.

Table I: Normalised Load supporting capability of distinct sliders when $l^* = 0.3, \ \delta = 1.5$

Sliders	M_0	C=0.0		C=0.2		C=0.4	
		Longitudinal	Transverse	Longitudinal	Transverse	Longitudinal	Transverse
Plane	0	0.174119	0.174119	0.172951	0.176597	0.169565	0.184684
	2	0.210969	0.210969	0.209853	0.213711	0.206609	0.222676
	4	0.29596	0.295959	0.29485	0.299255	0.291597	0.310049
Parabolic	0	0.197129	0.197129	0.195677	0.200216	0.191475	0.210331
	2	0.234079	0.234079	0.232722	0.237401	0.228786	0.248287
	4	0.322639	0.322638	0.321329	0.326518	0.317489	0.339241
Secant	0	0.184315	0.184315	0.182803	0.187538	0.178444	0.198174
	2	0.213987	0.213986	0.212598	0.217376	0.208581	0.228561
	4	0.28778	0.28778	0.286499	0.291591	0.282749	0.304158
Exponential	0	0.181074	0.181074	0.179851	0.183664	0.176295	0.19204
	2	0.21719	0.21719	0.216042	0.220016	0.212693	0.22917
	4	0.302265	0.302265	0.301145	0.305616	0.297847	0.316495

In Table II the computation of load supporting capability is calculated for roughness of surfaces by taking roughness parameter $C = 0.3$. It is noted that as the value of Hartmann number M_0 and couplestress parameter l^* increases the transverse as well as longitudinal load supporting capability of all sliders increases. It is found that parabolic slider is having superior load supporting capability.

Table II Normalised Load supporting capability of different sliders when $C = 0.3,\ \delta = 1.5$

Sliders	M_0	$l^* = 0.0$		$l^* = 0.2$		$l^* = 0.4$	
		Longitudinal	Transverse	Longitudinal	Transverse	Longitudinal	transverse
Plane	0	0.155951	0.162321	0.16315	0.1704240.2	0.182737	0.19245
	2	0.188728	0.195409	0.198267	05949	0.221611	0.231939
	4	0.258204	0.265739	0.276819	0.285579	0.313096	0.324971
Parabolic	0	0.127784	0.132196	0.183627	0.19262	0.207738	0.21996
	2	0.207865	0.215888	0.219028	0.2283	0.246628	0.259239
	4	0.280291	0.289133	0.301038	0.311345	0.341786	0.355792
Secant	0	0.122157	0.127132	0.170431	0.17972	0.195228	0.208162
	2	0.188127	0.196183	0.199027	0.208416	0.226433	0.239491
	4	0.248674	0.257275	0.267674	0.277748	0.305509	0.319375
exponential	0	0.161824	0.168548	0.169455	0.177088	0.190311	0.200412
	2	0.194061	0.201023	0.203982	0.211932	0.228357	0.23892
	4	0.263673	0.271429	0.282724	0.291673	0.319812	0.331747

Table III represent the changes in normalised frictional force of diverse sliders in the existence of couplestress fluid $l^* = 0.3$. The transverse frictional force coincides with longitudinal frictional force when the surface of bearing is smooth. It is found that the force of friction due to longitudinal roughness is higher than smooth case where as for vertical roughness the trend is reverse. It is found that as the value of Hartmann number and roughness parameter increases force of friction in parabolic slider is more significant.

Table III Normalised frictional force for distinct sliders when $l^* = 0.3,\ \delta = 1.5$

Sliders	M_0	C=0.0		C=0.2		C=0.4	
		Longitudinal	transverse	Longitudinal	Transverse	Longitudinal	transverse
Plane	0	0.743802	0.743802	0.748701	0.73707	0.763535	0.715611
	2	1.27234	1.27234	1.27643	1.26671	1.28898	1.24872
	4	2.38445	2.38445	2.38681	2.37841	2.39437	2.35957
Parabolic	0	0.853258	0.853258	0.863079	0.83907	0.892507	0.791986
	2	1.32475	1.32476	1.33365	1.31213	1.36054	1.26989
	4	2.38658	2.38658	2.39292	2.37354	2.41268	2.33055
Secant	0	0.888507	0.888507	0.901561	0.86938	0.940557	0.805432
	2	1.31834	1.31834	1.33044	1.30094	1.36688	1.2423
	4	2.33173	2.33173	2.3409	2.31368	2.36926	2.25356
Exponential	0	0.779896	0.779896	0.786451	0.770619	0.806192	0.740594
	2	1.28249	1.28249	1.2882	1.27444	1.30557	1.24826
	4	2.37319	2.37319	2.37687	2.36463	2.38d843	2.33726

Table IV shows the differences in frictional force when the surface are rough $(C = 0.3)$. It is evident that as the value of couplestress parameter and Hartmann number increases the force of friction in sliders increases. It is also observed for smaller values of l^* and M_0 the secant slider has more frictional force but as the value of l^* and M_0 increases the parabolic slider is having more frictional force.

Table IV Normalised frictional force for distinct sliders when $C = 0.3,\ \delta = 1.5$

Sliders	M_0	$l^* = 0.0$		$l^* = 0.2$		$l^* = 0.4$	
		Longitudinal	transverse	longitudinal	transverse	longitudinal	transverse
Plane	0	0.739629	0.71884	0.746675	0.723317	0.765915	0.734993
	2	1.24422	1.22734	1.26334	1.24404	1.30305	1.27675
	4	2.21326	2.19873	2.31133	2.29455	2.47263	2.4501
Parabolic	0	0.857531	0.817917	0.865747	0.81916	0.888419	0.821607

	2	1.30807	1.27363	1.32688	1.28561	1.36604	1.30512
	4	2.23209	2.20149	2.32705	2.28988	2.47694	2.42171
Secant	0	0.900127	0.847812	0.908276	0.846202	0.930935	0.840739
	2	1.31163	1.26499	1.32907	1.27276	1.36522	1.28127
	4	2.19386	2.15141	2.2839	2.23197	2.42155	2.34347
exponential	0	0.779489	0.752005	0.786499	0.755102	0.805739	0.762958
	2	1.25959	1.23641	1.27797	1.251	1.3158	1.27798
	4	2.2093	2.18885	2.30545	2.28139	2.46083	2.4272

Table V depicts the influence of roughness on coefficient of friction on distinct sliders. It is examined that due to transverse roughness pattern frictional coefficient decreases whereas due to longitudinal roughness striation trend is reversed. It is also analysed that as the value of parameters of roughness and MHD increases there is decrease in coefficient of friction of parabolic slider.

Table V Tabulated values for frictional coefficient corresponding to $l^* = 0.3,\ \delta = 1.5$

Sliders	M	C=0.0		C=0.2		C=0.4	
		Longitudinal	transverse	Longitudinal	transverse	Longitudinal	Transverse
Plane	0	4.2718	4.27181	4.32898	4.17375	4.5029	3.87479
	2	6.03092	6.03093	6.08252	5.92719	6.23872	5.6078
	4	8.05667	8.05668	8.095	7.94779	8.21123	7.61033
Parabolic	0	4.32842	4.32842	4.41074	4.19082	4.66122	3.76543
	2	5.65943	5.65944	5.73064	5.52706	5.94678	5.11459
	4	7.39707	7.39708	7.44695	7.26925	7.59924	6.86991
Secant	0	4.82059	4.82059	4.93186	4.63576	5.27087	4.06427
	2	6.16085	6.16086	6.25799	5.98474	6.55325	5.43533
	4	8.10247	8.10249	8.17071	7.93468	8.37938	7.40917
exponential	0	4.30705	4.30706	4.3728	4.19582	4.57296	3.85646
	2	5.90491	5.90492	5.96275	5.7925	6.13829	5.4469
	4	7.85134	7.85136	7.89277	7.73724	8.01898	7.38484

Table VI shows the consequence of couplestress and MHD in coefficient of friction on rough surface $(C = 0.3)$. When compared with other sliders, the parabolic slider's frictional coefficient decreases significantly as the value of l^*, M_0 increases.

Table VI Tabulated values of frictional coefficient of different sliders corresponding to $C = 0.3,\ \delta = 1.5$

Sliders	M_0	$l^* = 0.0$		$l^* = 0.2$		$l^* = 0.4$	
		Longitudinal	transverse	Longitudinal	transverse	Longitudinal	transverse
Plane	0	4.74268	4.4285	4.57662	4.24423	4.19134	3.81914
	2	6.59268	6.28087	6.37192	6.04051	5.87991	5.50468
	4	8.57173	8.27402	8.34963	8.03474	7.89738	7.53945
Parabolic	0	4.90513	4.47827	4.7147	4.25272	4.27663	3.73526
	2	6.29286	5.89948	6.05802	5.63124	5.53889	5.03441
	4	7.96347	7.61409	7.73009	7.3548	7.24704	6.80653
Secant	0	5.57502	5.00327	5.3293	4.70845	4.76844	4.03887
	2	6.97204	6.448	6.67783	6.10681	6.02923	5.34996
	4	8.82223	8.36229	8.53238	8.03595	7.92629	7.33767
exponential	0	4.81689	4.46167	4.64135	4.264	4.23381	3.80695
	2	6.49066	6.15058	6.26508	5.90284	5.76201	5.34898
	4	8.37892	8.06417	8.15445	7.82172	7.69461	7.31642

VI. CONCLUSION

Based on Christensen stochastic approach, and stokes couplestress fluid model, the modified Stochastic Reynolds equation with the collective impact of roughness, MHD and couplestress on the performance behaviour of different slider bearing has been presented in this paper. The characteristics of bearings are analysed numerically.

- It is concluded that the impact of MHD, couplestress and roughness enhances the load supporting capability, force of friction and reduces the frictional coefficient.
- From the comparison of different film shapes it is noted that the load supporting capability of parabolic slider is more significant
- It is expected that these analysis will help design engineers to choose proper shaped slider bearings with appropriate couplestress, roughness parameters in the occurrence of applied magnetic field, which enhances the life of the bearings.

VII. REFERENCES

[1] T. Ariman, M.A. Turk, N.D Sylvester., *" Microcontinuim fluid mechanics-a review*", Int. J of Engg Sci., Vol. 11 ,pp.905-930, 1973.

[2] T. Ariman, M.A Turk, N.D Sylvester., "*Application of microcontinuum fluid mechanics*", International journal of Engineering science, Vol. 12, pp 273-293, 1974..

[3] M.M Khonsari, D. E Brewe, "*On the performance of finite journal bearing lubricated with micropolar fluids*", Tribology transaction, Vol. 32, pp.155-160, 1989.

[4] V. K. Stokes., " Couplestresses in fluids", Physics of Fluids, Vol. 9, pp. 1709-1715, 1966.

[5] G Ramanaiah, P. Sarkar, "*Slider bearing lubricated by fluids with couple-stress*", Wear; Vol. 52, pp. 27-36, 1979.

[6] J.R.Lin, Yu-Ming Lu, "*Steady-state performance of wide parabolic shaped slider bearings with a couple stress fluids*", Journal of Marine science and Technology, Vol. 12, pp. 239-246,2004.

[7] Oladeinde, Mobolaji H Akpobi, A. John., *"Performance of Infinitely wide parabolic and inclined slider bearing lubricated with couplestress or magnetic fluids*", Proceedings on world congress on engineering, Vol. 1394, pp. 58-68, 2011.

[8] J.R Lin, C.R Hung, C.H Hsu, C Lai, *"Dynamic stiffness and damping characteristics of one dimensional MHD inclined-plane slider bearing"*, Proceedings of the institution of Mechanical engineers-part J Journal of engineering tribology, Vol. 223, pp. 211-219, 2009.

[9] J.R Lin, R.F Lu. "*Dynamic characteristics for magneto-hydrodynamic wide slider bearings with an exponential film profile*", Journal of marine science and technology, Vol.18, Issue.2, pp. 268-276, 2010.

NOMENCLATURE

B_0 applied magnetic field

c Maximum asperity deviation from nominal film height

C Dimensionless roughness parameter

d Inlet-outlet film thickness difference $(h_1 - h_0)$

F Frictional force

[10] J. R. Lin, *"Dynamic characteristics for wide magneto-hydrodynamic slider bearing with a power-law film profile*", Applied mathematical modelling, Vol. 36, pp. 4521-4528, 2012.

[11] Lin JR, *"MHD steady and dynamic characteristics of wide Tapered-Land Slider Bearings",* Tribology International, Vol. l 43, pp. 2378-2383, 2010.

[12] J. R Lin, R.F, Lu, T.C,Hung and L.J. Liang , *"Effects of magnetic fields on the dynamic characteristics of wide parallel step slider bearing with Electrically conducting Fluids*", Lubrication Science, Vol. 24, pp. 238-250, 2012.

[13] N.B Naduvinamani, S.T, Fathima, B.N.Hanumagowda., "Magnetohydrodynamic couplestress squeeze film lubrication of circular stepped plates", JET part J, Vol. 225, pp. 111-119, 2011.

[14] Biradar Kasinath, B. N Hanumagowda, "*MHD effect on composite slider bearing lubricated with couplestress fluids*", International journal of mathematics trends and technology, Vol. 5, pp. 27-49, 2014.

[15] S. T,Fathima, N. B Naduvinamani, H. M, Shivakumar B. N Hanumagowda, "*A Study on the Performance of Hydromagnetic Squeeze Film between Anisotropic Porous Rectangular Plates with Couple Stress Fluids*", Tribology Online, 9, pp. 1–9, 2014.

[16] S.T Fathima, N. B Naduvinamani, B.N Hanumagowda, J. Santhosh Kumar, *"Modified Reynolds Equation for Different Types of Finite Plates with the Combined Effect of MHD and Couple Stresses*", Tribology Transactions, Vol. 12, Issue.58:4, pp. 660-667, 2015.

[17] H. Christensen. "*Stochastic models for hydrodynamic lubrication of rough surfaces*", Proc of the Inst of Mechanical Engineers part I, ,Vol. 184, pp. 1013-1026, 1969.

[18] N.B. Naduvinamani, A Siddanagouda, *"Effect of surface roughness on the hydrodynamic lubrication of porous step-slider bearings with couplestress fluids",* Tribology International, Vol. 40, pp. 780-793, 2007.

[19] N.B. Naduvinamani, ST, Fathima , P. S. Hiremath, " *On the squeeze effect of lubricants with additives between rough porous rectangular plates"*, ZAMM, Vol.84, pp. 825-834, 2004.

[20] N.B. Naduvinamani, B. N. Hanumagowda, S. T Fathima. "*Combined effects of MHD and surface roughness on couple-stresss squeeze film lubrication between porous circular stepped plate*", Tribology International, Vol. 56, pp. 19-29, 2012.

[21] N.B. Naduvinamani, P.S Hiremath, G Gurubasavaraj, *"Effect of surface roughness on the couplestress squeeze film between a sphere and a flat plate,"* Tribology International, Vol. 38, pp. 451-458, 2005.

[22] N.B. Naduvinamani, P. S Hiremath, G. Gurubasavaraj, *" Surface roughness effects in a short porous journal bearing with a couple stress fluid",* Fluid Dynamic Research, Vo.31, Issue.6, pp. 315-316, 2002.

[23] N.B. Naduvinamani., S.T Fathima, P.S. Hiremath., "*Hydrodynamic lubrication of rough slider bearings with couplestress fluids*", Tribology International, Vol. 36, Issue.12, pp. 949-959, 2003.

F^* Non-dimensional frictional force $\left(=-Fh_0/\mu UL\right)$

H Film thickness

h_s Stochastic film thickness

h_1 Inlet film thickness

h_0 Outlet film thickness

H^* Non-dimensional film thickness $\left(H/h_0\right)$

l Couplestress parameter

l^* Non-dimensional couplestress parameter

L Bearing length

M_0 Hartmann number

p Pressure in the film region

P Non-dimensional pressure

x, y Rectangular co-ordinates

x^* Non-dimensional rectangular coordinates $\left(=x/L\right)$

u, v Velocity component in film region

w Load carrying capacity

W^* Non-dimensional load carrying capacity $\dfrac{E(w)h_0^2}{\mu UL^2}$

δ Non-dimensional inlet-outlet thickness difference $\left(=d/h_0\right)$

η Material constant characterizing couple stress

μ Viscosity coefficient

σ Electrical conductivity

χ Coefficient of friction

